Reactive and Kinetic Properties of Carbon Monoxide and Carbon Dioxide on a Graphite Surface

B. Marchon,*,† W. T. Tysoe,†,‡ J. Carrazza,†,§ H. Heinemann,†,⊥ and G. A. Somorjai†,§

Materials and Chemical Sciences Division, Lawrence Berkeley Laboratory, Department of Chemistry, and Department of Chemical Engineering, University of California, Berkeley, California 94720
(Received: November 3, 1987; In Final Form: March 10, 1988)

Temperature-programmed desorption (TPD) results after chemisorption of carbon monoxide (CO) and carbon dioxide (CO_2) on polycrystalline graphite are presented. CO adsorbs onto graphite with a very low sticking coefficient. After CO chemisorption, CO (mass 28 amu) desorbs in two temperature regions, between 400 and 700 K and between 1000 and 1300 K, and CO_2 (mass 44 amu) desorbs below 950 K. The intensity of the CO_2 signal is less than 1 order of magnitude lower than the CO intensity. After CO_2 adsorption the major desorption product is CO at high temperatures ($1000 < T$ (K) < 1300), whereas a small amount of CO_2 desorbs around 450 K. The adsorption of a $C^{16}O_2$ and $C^{18}O_2$ mixture leads to a nearly total oxygen scrambling of the CO_2 desorbed. A mechanism for CO and CO_2 interconversion on the graphite surface is presented in terms of surface oxide species, mainly lactones and semiquinones, and their relative stability. Assignments of the TPD features are proposed accordingly. Reaction studies on the CO_2 gasification of clean graphite and the CO disproportionation (Boudouard reaction) have been performed. A good agreement is found between the activation energies obtained and the desorption energies calculated from the analysis of the TPD results.

Introduction

The surface oxides of a variety of carbon compounds such as carbon black, carbon fibers, coal, and graphite have been extensively studied over the past 2 decades by an array of different methods. pH measurements,[1] reactor studies,[2] chemisorption kinetics,[3,4] optical microscopy,[5] thermal desorption under atmospheric pressure,[6-13] and more recently new techniques such as infrared absorption[14,15] and nuclear magnetic resonance (NMR)[16] and surface science tools such as X-ray photoelectron spectroscopy (XPS),[17-19] Auger electron spectroscopy (AES),[20,21] and temperature-programmed desorption (TPD)[20-22] have brought some useful information on the nature of these surface species.

Most papers have dealt with the natural surface oxides or have studied oxidation of the clean surface (obtained after degassing at high temperatures) by O_2 or CO_2. All of them report a strongly bound surface complex that desorbs at temperatures higher than 1100 K as CO.

The nature of this oxide is not yet well understood, although some evidence for a semiquinone group has been observed.[15,19] Other groups such as carboxyls and lactones have also been proposed as possible candidates for graphite surface oxides.[1,2,11,14]

To our knowledge, no work has been published on CO adsorption on graphite edge surfaces. The approach of this work has been to study the species produced by the chemisorption of CO and CO_2 and their isotopic derivatives labeled with ^{13}C and ^{18}O onto a clean graphite sample under ultrahigh vacuum (UHV) conditions. This permits the resulting surface species to be examined by using a surface-sensitive probe such as temperature-programmed desorption. Experiments have been carried out on graphite samples from three different origins to check the reproducibility of the results. Also, kinetic measurements have been undertaken to study the interconversion of CO and CO_2 at the graphite surface (Boudouard equilibrium).

Experimental Section

For maximization of the number of edge sites (which are the active chemisorption sites), three different kinds of finely dispersed polycrystalline graphite were used: two of them were commercial suspensions, one in isopropyl alcohol (Electrodag) and the other in water (Aquadag). The third sample was sintered machinable graphite that was finely ground and dispersed in hexane.

None of these samples is expected to be of maximum purity since they all contain a small amount of binder. However, the binder is organic and very diluted. It is therefore likely to decompose at high temperatures. No metallic impurities are reported for either Aquadag or Electrodag suspensions. Their surface area is approximately 3 m^2/g, with an average grain diameter of 1 μm.

About 5 mg (once dried) of these suspensions was coated as thin films on a piece of tantalum foil. Tantalum was chosen for its high melting point (3269 K), low vapor pressure, and good mechanical properties and because it is covered with a very inert passivating oxide layer. The noncatalytic properties of tantalum toward graphite gasification were checked by running a reaction under flow reactor conditions with water vapor at 900 K. No carbonaceous compounds evolved. Blank TPD experiments were also carried out on the foil, without graphite, and no significant amount of CO or CO_2 adsorbed on the surface.

The sample was cleaned by annealing at ca. 1500 K for about 60 s. Neither XPS nor AES spectra showed an oxygen signal after the treatment. CO and CO_2 gases were of standard purity, and the ^{13}C- and ^{18}O-enriched compounds from Cambridge Isotope Laboratories were 98% pure.

* To whom correspondence should be addressed at Laboratoire de Spectrochimie Infrarouge et Raman, CNRS, 94320 Thiais, France.
† Lawrence Berkeley Laboratory.
‡ Permanent address: Department of Chemistry, University of Wisconsin, Milwaukee, WI 53211.
§ Department of Chemistry.
⊥ Department of Chemical Engineering.

(1) Fabish, T. J.; Schleifer, D. E. *Carbon* **1984**, *22*, 19.
(2) Koenig, P. D.; Squires, R. G.; Laurendeau, N. M. *Carbon* **1985**, *23*, 531.
(3) Hart, P. J.; Vastola, F. J.; Walker, P. L. *Carbon* **1967**, *5*, 363.
(4) Bansal, R. C.; Vastola, F. J.; Walker, P. L. *J. Colloid Interface Sci.* **1969**, *32*, 187.
(5) Marsh, H.; O'Hair, T. E. *Carbon* **1969**, *7*, 703.
(6) Bonnetain, L. *J. Chim. Phys. (Les Ulis, Fr.)* **1961**, *58*, 34.
(7) Vastola, F. J.; Hart, P. J.; Walker, P. L. *Carbon* **1964**, *2*, 65.
(8) Dollimore, J.; Freedman, C. M.; Harrison, B. H.; Quinn, D. F. *Carbon* **1970**, *8*, 587.
(9) Tucker, B. J.; Mulcahy, M. F. R. *Trans. Faraday Soc.* **1969**, *65*, 274.
(10) Feates, F. S.; Keep, C. W. *Trans. Faraday Soc.* **1970**, *66*, 3156.
(11) Barton, S. S.; Boulton, G. L; Harrison, B. H. *Carbon* **1972**, *10*, 395.
(12) Sen, A.; Bercaw, J. E. *J. Phys. Chem.* **1980**, *84*, 465.
(13) Britten, J. A.; Falconer, J. L.; Brown, L. F. *Carbon* **1987**, *23*, 627.
(14) Ishizaki, C.; Marti, I. *Carbon* **1981**, *19*, 409.
(15) Akhter, M. S.; Keifer, J. R.; Chughtai, A. R.; Smith, D. M. *Carbon* **1985**, *23*, 589.
(16) Mims, C. A.; Rose, K. D.; Melchior, M. T.; Pabst, J. K. *J. Am. Chem. Soc.* **1982**, *104*, 6886.
(17) Perry, D. L.; Grint, A. *Fuel* **1983**, *62*, 1024.
(18) Clark, D. T.; Wilson, R. *Fuel* **1983**, *62*, 1034.
(19) Tagahagi, T.; Ishitani, I. *Carbon* **1984**, *22*, 43.
(20) Kelemen, S. R.; Freund, H. *Carbon* **1985**, *23*, 619.
(21) Kelemen, S. R.; Freund, H. *Carbon* **1985**, *23*, 723.
(22) Barton, S. S.; Harrison, B. H.; Dollimore, J. *J. Phys. Chem.* **1978**, *82*, 290.

0022-3654/88/2092-5744$01.50/0

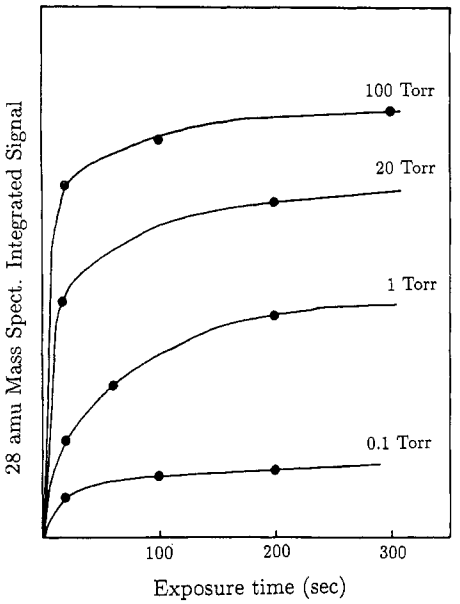

Figure 1. CO adsorption kinetics on polycrystalline graphite at room temperature. The CO coverage is estimated from the integrated intensity of the 28 amu low-temperature TPD peak.

The experiments were performed in a stainless-steel diffusion-pumped ultrahigh vacuum chamber. Additional titanium sublimation pumping allowed a base pressure of 5×10^{-10} Torr to be obtained after bakeout. Repeated adsorption–desorption cycles, however, led to working base pressures of 2×10^{-9} Torr.

The sample was mounted on a rotatable manipulator. It could be resistively heated, and the temperature measured by means of a chromel–alumel thermocouple in intimate contact with the sample. A coaxial high-pressure reactor was incorporated into the chamber so that the sample could be isolated from UHV and exposed to a high pressure (up to 760 Torr) of CO or CO_2. The gases were circulated around an external loop to ensure that the reactants and products were well homogenized. It was found indispensible to bake out the loop for at least 1 h before any gas introduction to avoid contamination by residual H_2O and O_2.

The rotatable manipulator allowed the sample to be turned toward a quadrupole mass spectrometer located 5 cm away from the sample for thermal desorption studies. TPD experiments were carried out by using a heating rate of 50 K/s. Such a rate, together with the broadness of our TPD peaks, leads to a precision on the desorption temperatures of ca. 10 K.

In the kinetic studies, the reaction mixture was analyzed by using a gas chromatograph equipped with a thermal conductivity detector sensitive to both CO and CO_2.

Results

The three different samples described above yielded similar results, although slight differences in TPD peak intensities were observed. Only results for the Aquadag samples will therefore be presented.

CO Adsorption. The CO adsorption kinetics are presented in Figure 1. The total CO desorption measured by integrating the mass 28 amu TPD peak is plotted versus exposure at various pressures.

The thermal desorption spectra taken after adsorption of 6×10^{-5} Torr of CO for 30 s at different temperatures are plotted in Figure 2. When adsorption takes place at 323 K, CO desorption occurs in two overlapping peaks at 393 and 503 K. Adsorption at higher temperatures yields other TPD peaks at 673, 973, and 1093 K. Similar adsorption of ^{13}C showed no ^{12}CO evolved, i.e., no carbon exchange with the bulk occurs. Also, this allows us to rule out any O_2 or H_2O contaminations, which would lead to ^{12}CO desorption. Additional experiments performed with $C^{18}O$ confirmed this observation.

It is important at this point to address the question of the purity of the graphite sample and the possible preferential adsorption

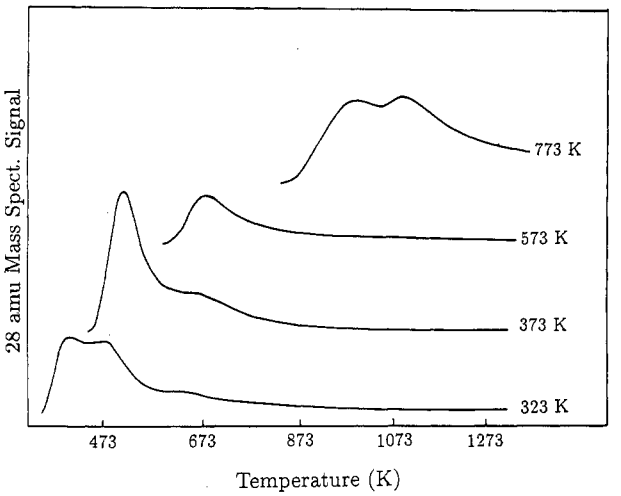

Figure 2. TPD spectra, mass 28 amu, after CO adsorption (6×10^{-5} Torr for 30 s) on polycrystalline graphite at various temperatures.

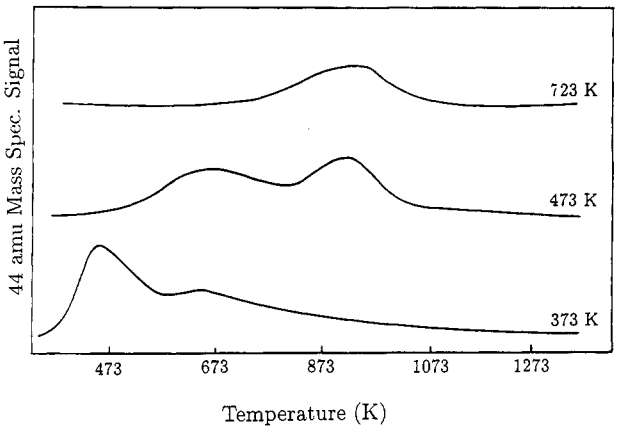

Figure 3. TPD spectra, mass 44 amu, after CO adsorption (6×10^{-5} Torr for 30 s) on polycrystalline graphite at various temperatures.

of CO on impurity sites. As we said earlier, no metallic impurities are reported for the Aquadag suspension. If we assume, however, their concentration to be of the order of 10 ppm in a total amount of graphite of 5 mg, this will lead to a number of metal atoms of the order of 2.5×10^{15}. This is the same order of magnitude as the total number of the surface atoms on our 1-cm^2 tantalum foil (approximately 10^{15}). Blank experiments we carried out on this foil have shown that it does not participate significantly in CO chemisorption. Therefore, we believe that our TPD data result from adsorption on the graphite surface and not on impurity sites. The similarity of the results obtained from the three graphite samples of different origins brings an additional indication that the role of such impurities is negligible.

Some CO_2 (mass 44 amu) is produced after CO adsorption (Figure 3). Room-temperature adsorption leads to a single peak at 443 K, whereas higher adsorption temperatures lead to more stable species that desorb at 673 and 923 K. In our experimental conditions the amount of CO_2 desorbed after CO adsorption is always less than 10% of the total amount of CO chemisorbed.

CO_2 Adsorption. The TPD spectra for mass 28 (^{12}CO), 29 (^{13}CO), 44 ($^{12}CO_2$), and 45 amu ($^{13}CO_2$) after adsorption of 8 Torr of $^{13}CO_2$ for 60 s at room temperature are reproduced in Figure 4. Molecular $^{13}CO_2$ desorbs at 423 K. A large high-temperature ^{12}CO TPD peak at 1093 K with two shoulders at 923 and 1253 K is observed. $C^{18}O_2$ adsorption resulted in identical desorption peaks at mass 30 amu ($C^{18}O$), indicating that there is no O_2 or H_2O contamination. Some ^{13}CO (mass 29 amu) is evolved at low temperature, and the weak mass 44 amu signal ($^{12}CO_2$) can be ascribed to isotopic impurities.

Adsorption of a mixture of 58% $C^{16}O_2$–42% $C^{18}O_2$ leads to a nearly total scrambling on the surface as the CO_2 desorbed is 35% $C^{16}O_2$ (mass 44 amu), 41% $C^{16}O^{18}O$ (mass 46 amu), and 24%

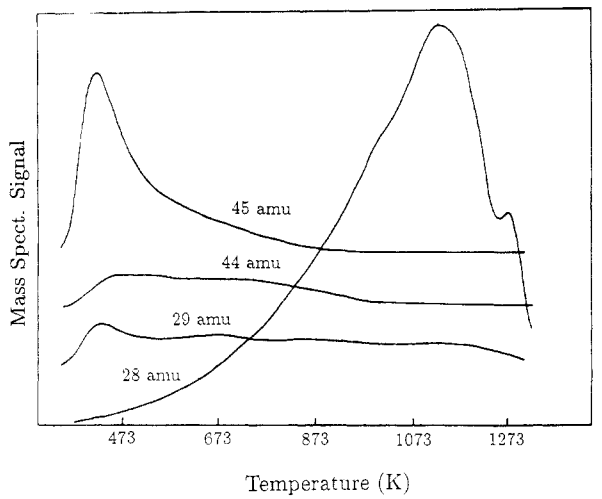

Figure 4. TPD spectra after $^{13}CO_2$ adsorption (8 Torr for 60 s) on polycrystalline graphite at room temperature.

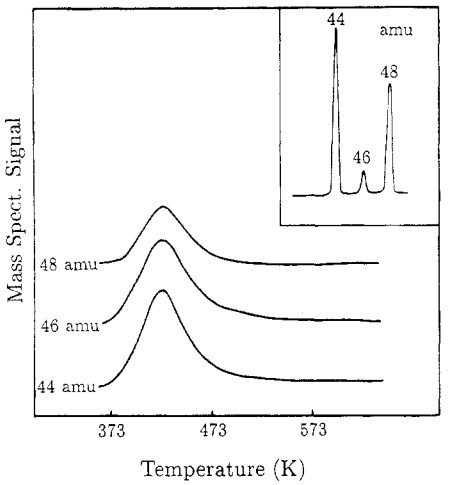

Figure 5. TPD spectra after adsorption (2×10^{-4} Torr for 30 s) of a 58% $C^{16}O_2$–42% $C^{18}O_2$ mixture on polycrystalline graphite at room temperature. In the insert is the mass spectrum of the mixture; the mass 46 amu peak is ascribed to an isotopic impurity.

$C^{18}O_2$ (mass 48 amu) (Figure 5). Theoretical proportions for total scrambling are 34, 48, and 18%, respectively.

Kinetic Results. Reaction rates between CO and graphite and CO_2 and graphite were obtained by using the high-pressure reactor. Data for the $C + CO_2 \rightarrow 2CO$ reaction as a function of temperature (plotted in Arrhenius form) are shown in Figure 6. The slope of this line yields an activation energy of 67 ± 3 kcal/mol. This value is slightly lower than what has been previously reported in the literature (70–90 kcal/mol).[23]

Figure 7 shows a similar plot for the reverse reaction: $2CO \rightarrow C + CO_2$. In this case, rates were measured from the accumulation of CO_2, and the linear portion of the curve yields an activation energy for CO_2 formation of 24 ± 2 kcal/mol.

Discussion

CO adsorbs onto graphite with a very low sticking coefficient. The mass 28 amu TPD peak obtained after adsorption of 100 Torr of CO for 30 s is 1 order of magnitude smaller than the one obtained after O_2 adsorption.[24] Since it is well established that chemisorbed oxygen covers only a few percent of the total number of surface carbon atoms,[3,6,22] it is clear that CO adsorption on graphite is a very low probability event, that is, it is highly activated. Its sticking probability is difficult to estimate, since the exact number of chemisorption sites in our polycrystalline sample

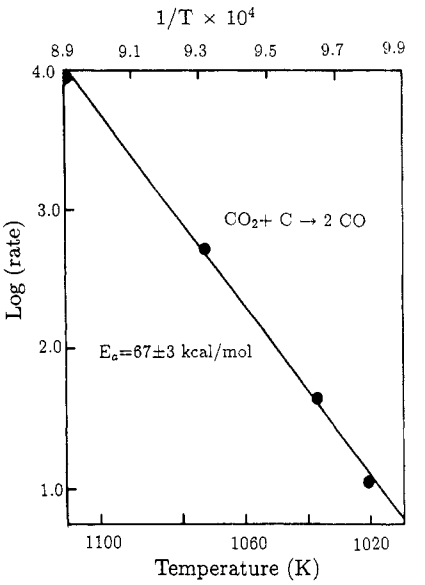

Figure 6. Arrhenius plot for the reaction $C + CO_2 \rightarrow 2CO$ performed in the high-pressure cell.

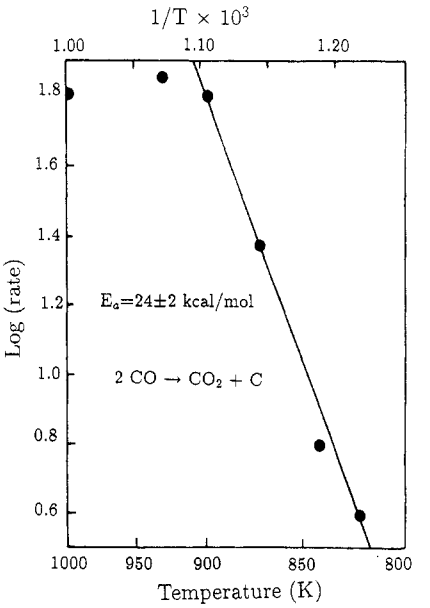

Figure 7. Arrhenius plot for the reaction $2CO \rightarrow C + CO_2$ performed in the high-pressure cell.

is unknown. It will not be discussed here.

Figure 2 shows that CO (mass 28 amu) desorbs in two temperature regions after CO adsorption. When CO is adsorbed at room temperature, desorption peaks at 393, 503, and 673 K are obtained, and when CO is adsorbed above 800 K, TPD peaks at 973 and 1093 K are observed. These results suggest that the two temperature regions are due to the desorption of two distinct surface species. The high-temperature TPD feature is also observed after CO_2 adsorption (Figure 6) and O_2 or H_2O oxidation,[24] and it is therefore likely due to the same species. CO desorption peaks from carbon in the low-temperature region have not been reported after adsorption of O_2, CO_2, or H_2O, but desorption of CO from metal surfaces usually occurs in this temperature region (400–700 K),[25] which may indicate that the same type of chemisorbed species is formed in both cases.

Figure 4 shows that the major desorption product after CO_2 adsorption is CO at high temperatures. This figure also shows that the adsorption of $^{13}CO_2$ favors the desorption of ^{12}CO. This indicates the dissociation of CO_2 and the creation of a carbon–

(23) Strange, J. F.; Walker, P. L. *Carbon* **1976**, *14*, 345.
(24) Marchon, B.; Carrazza, J.; Heinemann, H.; Somorjai, G. A. *Carbon* **1988**, *26*, 507.
(25) Somorjai, G. A. *Chemistry in Two Dimensions: Surfaces*; Cornell University Press: Ithaca, NY, 1981.

TABLE I: Desorption Products and Energies of Desorption of CO and CO_2 Adsorbed on Graphite

adsorption gas	adsorption temp, K	desorption product	desorption temp, K	E_{des}, kcal/mol	assignment
CO	>800	CO	973–1253	64–83	semiquinones
CO_2	room temp	CO	973–1253	64–83	semiquinones
CO	325–600	CO	400–700	25–44	carbonyls
CO	room temp	CO_2	443	28	lactones
CO_2	room temp	CO_2	423	27	lactones
CO	400–750	CO_2	443–923	28–60	lactones

oxygen bond from the graphite lattice, which would eventually desorb as ^{12}CO at high temperatures. This agrees with the mechanism proposed earlier by several authors:[2,9,13]

$$^{13}CO_2 + {}^{12}C \rightarrow {}^{12}C_s(O) + {}^{13}CO\uparrow \quad (1)$$

where the $^{12}C_s(O)$ is likely to be the same strongly bound species that is obtained after CO adsorption at high temperature (Figure 2), owing to the similar desorption temperature. Reaction 1 implies the release of ^{13}CO, which can further adsorb on the surface. This is, however, a very low probability process, as discussed previously, and for this reason the area of the mass 29 amu peak in Figure 6 is much lower than that of the mass 28 amu peak.

Activation energy for desorption can be deduced from a TPD experiment, and this has been extensively discussed by Falconer and Shwarz.[26] In particular, a line-shape analysis of a TPD peak for a simple process, a first-order desorption reaction, can lead to its activation energy, when the preexponential factor is unknown. In our case, however, the likely presence of a multicomponent desorption process, due to the participation of several desorption sites, makes such an analysis impossible. We will therefore prefer the less accurate but simpler peak position method by Redhead,[27] assuming a frequency factor close to 10^{13} s^{-1}.[23] The values obtained for the CO and CO_2 species observed are summarized in Table I. The activation energy for CO_2 gasification (67 kcal/mol) agrees well with that at the lowest desorption temperature for CO formation after CO_2 adsorption (around 64 kcal/mol), and the activation energy for the Boudouard reaction (24 kcal/mol) coincides with the lower limit in activation energy for desorption of CO_2 after CO adsorption (28 kcal/mol). This would indicate that both reactions are controlled by the decomposition of the surface species. This is in contradiction, however, with earlier studies showing that CO_2 gasification was adsorption controlled.[28] Further experiments are needed to clarify this point, but it is likely that both adsorption and desorption are important factors in the determination of the reaction rate.

As mentioned in the Introduction, there has been a great number of studies on the surface oxides adsorbed on various types of carbons. These studies, including spectroscopy, have proposed the existence of several types of surface groups. In what follows, we will discuss in more detail what chemical surface species are formed on the graphite surface after CO or CO_2 adsorption and that are responsible for the TPD peaks. As previously discussed, analysis of TPD data provides information about the desorption energy of the surface species involved, which is related to the strength of the bonds involved in the desorption process. By comparing these values with bond energies in similar organic compounds, we can make tentative assignments of the various desorption features to surface species.

It should be noticed, however, that it is difficult to get precise values of the bond energies on the graphite surface, from the desorption energies obtained from TPD. First, desorption energies are the sum of the activation energy for adsorption and the surface bond energy. This activation energy for adsorption is very low in the case of CO desorption on metal surfaces, for instance,[25] but is known to be of the order of 10 kcal/mol[4] or greater[20] for O_2 on graphite. Also, Sanderson has pointed out[29] that the reorganizational energy of radicals after breaking the surface bond is an important contribution to the desorption energy, and in graphite this energy is expected to be considerable, because of the electron delocalization. Another complication to the determination of the bond strengths from TPD experiments is that the edges of the graphite particles contain various adsorption sites (zig-zag, arm-chair, etc.)[30] that lead to species of different stability, whose desorption will multiply or at least broaden the TPD features. For example, theoretical calculations[31] have shown that arm-chair sites are less reactive than zig-zag sites but are more stable.

Despite the complexity of the surface structure and the large number of variables involved in the desorption energy, we can reasonably assume that each surface species is likely to desorb in the same temperature range and that some qualitative trends can be established, which can help in the assignment of the TPD features to particular surface species. For example, it is easier to break external carbon–carbon bonds (~80 kcal/mol) than internal graphitic ones (~115 kcal/mol), and at temperatures below 1500 K, carbon–oxygen single bonds can be thermally dissociated (~85 kcal/mol), but double bonds cannot (~175 kcal/mol).

Taking into account all these considerations, the TPD features observed are assigned as follows. The low-temperature CO desorption peaks at 393, 503, and 673 K, after exposure to CO at room temperature (Figure 2) are likely due to weakly bound species such as carbonyl and/or cyclic ether groups:

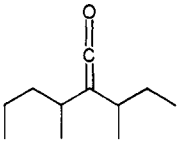

carbonyl

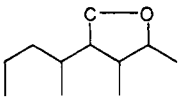

ether

To our knowledge, carbonyl species adsorbed on carbon have never been cited in the literature before, but analogy with CO adsorption on single-crystal metal surfaces[25] makes them favorable candidates. The transformation into ether groups is only a ring closure and appears energetically favored. The lack of spectroscopic data, however, prevents any further answer. The mass 28 amu high-temperature peaks between 923 and 1123 K, obtained after CO adsorption above 800 K, and CO_2 adsorption can be assigned to semiquinone species adsorbed on various sites, like on a zig-zag edge as shown here:

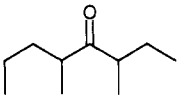

semiquinone

The high stability of quinone groups in polycyclic aromatic compounds[32] gives strong support to the existence of semiquinones on the graphite surface. The desorption of this species involves the breaking of two graphitic carbon–carbon bonds from the lattice and explains the high desorption temperature. In the case of ^{13}CO

(26) Falconer, J. A.; Shwarz, J. L. *Catal. Rev. Sci. Eng.* **1983**, *25*, 141.
(27) Redhead, P. A. *Vacuum* **1962**, *12*, 203.
(28) Biederman, D. L.; Miles, A. J.; Vastola, F. J.; Walker, P. L. *Carbon* **1976**, *14*, 351.
(29) Sanderson, R. T. *Chemical Bond in Organic Compounds*; Sun and Sand: Scottsdale, AZ, 1976.
(30) Smith, R. N.; Young, D. A.; Smith, R. A. *Trans. Faraday Soc.* **1966**, *62*, 2280.
(31) Stein, S. E.; Brown, R. L. *Carbon* **1985**, *23*, 105.
(32) Clar, E. *Polycyclic Aromatic Hydrocarbons*; Academic: New York, 1964.

SCHEME I

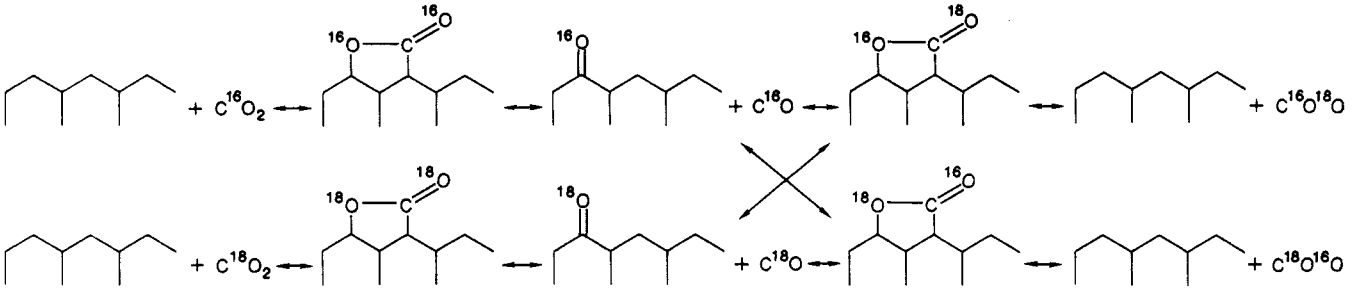

adsorption at high temperature, no ^{12}CO is evolved, indicating that CO does not dissociate on the surface, but rather it inserts onto the graphite lattice following the possible mechanism

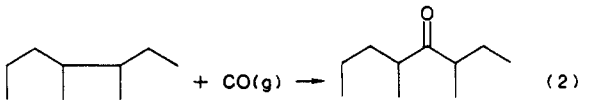

(2)

This insertion requires the presence of a five-membered ring, which has already been documented,[21] and the scission of its external carbon–carbon bond. It explains why its formation is such a highly activated process.

At this point it is important to make a comment about the nomenclature used to identify these species. The name carbonyl has been employed to identify the low-temperature CO species, rather than ketene, in agreement with IUPAC rules.[33] It must not be confused with the CO species desorbing above 1000 K after CO or CO_2 adsorption. Most authors refer to this highly stable species as carbonyl, but we prefer a more specific denomination, such as ketone or oxo[34] or, better, semiquinone,[35] to emphasize the strong conjugation with delocalized electrons as encountered in quinoid structures.

The formation of a semiquinone group from CO_2 follows the previously described reaction (1), where the surface complex $C_s(O)$ is now better characterized:

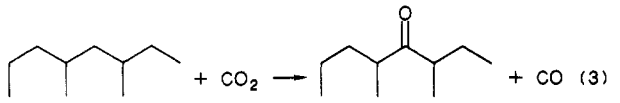

(3)

The desorption of CO_2 at 443, 673, and 923 K after CO adsorption is likely due to the thermal decarboxylation of a lactone group, which is a well-known organic reaction taking place in the same temperature range.[36] The formation of these lactone functionalities from CO may imply semiquinone groups as intermediates (eq 4).

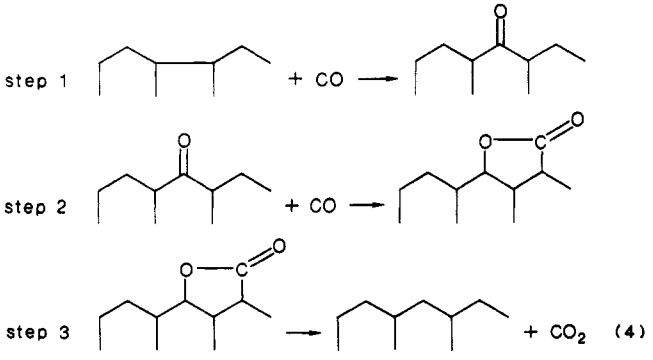

(4)

Again, a number of different sites are likely to give rise to such chemical species, and this explains the existence of several TPD

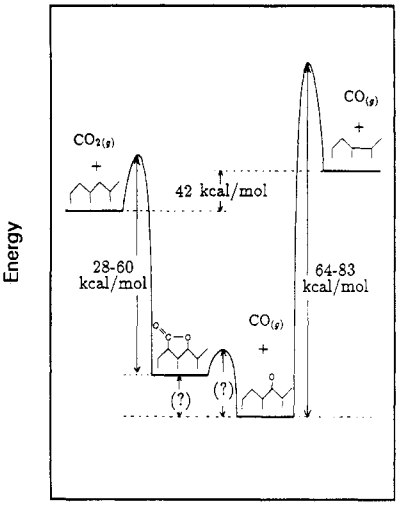

Figure 8. Simplified model for CO and CO_2 interconversion on a graphite surface. Some energy ranges deduced from our experiments are indicated. The enthalpy for the Boudouard reaction (42 kcal/mol) is from ref 38. The ordinate units are arbitrary, and the relative energy levels of the surface compounds are not respected.

44 amu peaks in the low-temperature region.

Equation 3 is simply the reverse reaction of eq 4 from step 3 to step 1, where step 2 has been omitted. The large number of semiquinone groups formed after CO_2 adsorption as compared to lactones (Figure 4) shows their greater stabilities as graphite surface species. The total oxygen scrambling that occurs when CO_2 is adsorbed (Figure 5) may be explained by the kinetic equilibrium between the semiquinone and the lactone groups of eq 4 and can be illustrated as shown in Scheme I.

A summary of CO and CO_2 interconversion on the surface of graphite is shown in Figure 8.

Other chemical groups such as carbonates have been proposed as graphite surface oxides[14] and could account for the isotope scrambling as well. Such carbonates exist on a number of metal oxide surfaces[37] and are reasonable candidates for existing on the surface of graphite. At this point, we cannot rule out such species, and more spectroscopic data should be gathered to clarify this. However, owing to the complexity of the system and the simplicity of our model which accounts for the experimental data, we will not discuss the existence of more elaborated structures.

Summary

The chemisorption and kinetic properties of CO and CO_2 adsorbed on graphite have been studied. Adsorption of CO is a highly activated process. It desorbs in two temperature regions, between 400 and 700 K and between 1000 and 1200 K, suggesting the formation of two distinct groups of surface species, carbonyls and semiquinones, respectively. After adsorption of CO_2, CO is

(33) IUPAC, *Nomenclature of Organic Chemistry*; Pergamon: New York, 1979; Rule C321.2.
(34) Reference 33, Rule C.3.1.
(35) Garten, V. A.; Weiss, D. E.; Willis, J. B. *Aust. J. Chem.* **1957**, *10*, 295.
(36) Adam, W.; Baeza, J.; Liu, J. C. *J. Am. Chem. Soc.* **1972**, *94*, 2000.
(37) Hair, M. L. *Infrared Spectroscopy in Surface Chemistry*; E. Arnold: Baltimore, 1967; p 204.
(38) *Handbook of Chemistry and Physics*, 64th ed. CRC Press: Boca Raton, FL, 1983.

the main desorption product. Its desorption temperature is similar to that of the high-temperature CO peak obtained after CO adsorption. This suggests that the same surface species, a semiquinone, is formed in both cases. In the CO case this species is formed by incorporation of the CO in the graphite lattice, while in the CO_2 case it is formed by dissociation of CO_2 and transfer of one oxygen atom from the adsorbed gas onto the graphite lattice.

In both cases of CO and CO_2 adsorption at room temperature, CO_2 is desorbed between 423 and 443 K. In the CO case the amount of CO_2 desorbed is less than 10% of the amount of CO chemisorbed. In the CO_2 case the adsorption of a $C^{16}O_2$ and $C^{18}O_2$ mixture leads to a nearly total oxygen scrambling of the CO_2 desorbed. Surface lactone functionalities are proposed to account for this behavior.

We have evidence of various chemisorption sites (zig-zag, arm-chair, etc.) for a given surface species, according to several different TPD peak temperatures.

Reaction studies on the CO_2 gasification and CO disproportionation (Boudouard reaction) have been performed. A comparison between the activation energies obtained and the desorption energies calculated from the analysis of the TPD results indicates that both reactions are strongly dependent on the desorption of the products, i.e., the decomposition of the surface species.

Acknowledgment. This work was supported by the Assistant Secretary for Fossil Energy, Office of Management Planning and Technical Coordination, Technical Division of the U.S. Department of Energy under Contract No. DE-AC03-76SF00098, through the Morgantown Energy Technology Center, Morgantown, WV 26505. J.C. acknowledges CEPET of Venezuela for a research fellowship.

Registry No. CO, 630-08-0; CO_2, 124-38-9; graphite, 7782-42-5.

Yield of Exoelectrons from Cluster Bombardment of Metallic Surfaces

Pieter J. De Lange, Peter J. Renkema, and Jan Kommandeur*

Laboratory for Physical Chemistry, Nijenborch 16, 9747 AG Groningen, The Netherlands
(Received: November 19, 1987; In Final Form: April 19, 1988)

Electron emission is observed when a neutral supersonic cluster beam collides with a metallic surface. Using a simple theoretical model based on thermionic emission, we compare calculated electron yields with measured yields for several cluster distributions. This is done for two different collision models. Surprisingly, we have to use a very low value of the heat conductivity to fit the experimental result of reaching surface temperatures of about 5000 K.

Introduction

During the past few years there has been a growing interest in the formation and the properties of molecular clusters.[1] Experiments have been performed with clusters of organic molecules[2-4] as well as with metallic clusters.[5] The properties of clusters are exceedingly interesting because they form aggregates that can be thought of as intermediate between the solid, the liquid, and the gas phase.

One of the easiest ways to generate clusters is the supersonic expansion of a vapor through a nozzle into a vacuum.[5] Mostly the vapor is seeded into a carrier gas, e.g., helium or argon, to have more collisions during the expansion and by this to obtain an effective cooling of the vapor. The yield of large clusters can be further increased by using a nozzle equipped with a conical headpiece, which extends the collision region.[4,6]

The size distribution of the clusters can be analyzed by a mass spectrometer, but one has to be careful with the interpretation because ionization can give rise to fragmentation of the cluster ion. In case of "large" clusters (more than 50 molecules per cluster), ionized by photons with an energy just above the ionization potential, we do not expect dramatic fragmentation effects, because of the enormous heat bath formed by the van der Waals bonds where the excess energy can be absorbed.

A recently discovered effect is the ejection of electrons from a metallic surface upon bombardment by molecular clusters formed in a supersonic jet expansion.[7] They were called exoelectrons. The kinetic energy of clusters that are seeded into helium is so high that when it is possible to transfer (part of) this energy to a metallic surface, an area becomes locally so highly excited that electron emission may result. The kinetic energy distribution of these so-called exoelectrons was measured for bombardment of various metals (copper, aluminum, nickel) with CCl_4 clusters. The curve that was obtained can be described by a steep rise at zero electron energy and an exponential falloff. From the exponent a local surface temperature of 5000 K was derived, essentially independent of the metal. From comparison of the result with experiments in which a metal is bombarded by slow noble-gas ions[8] there are notable differences. The electron energy distributions measured in those experiments show structure that depends strongly on the metal. It is described by a radiationless, two-electron, Auger-type transition, which neutralizes the ion to its ground state at the metal surface and simultaneously excites another electron in the solid. The collision of a neutral cluster with a metal excites a much larger area of the surface, so more electrons of the metal will be involved. Therefore, ejected electrons do not "remember" the energy of the cluster, and there is no structure in the kinetic energy distribution of the electrons.

The total number of electrons emitted depended strongly on the cluster size distribution, hardly or no electron emission for low expansion pressures (generating small clusters, less than 50 molecules per cluster) and many electrons for high expansion pressures (generating large clusters), while the beam velocity did not change significantly. No exoelectron emission was observed when clusters of organic molecules collided with a metallic surface and argon was used as carrier gas. Although the cluster distribution shifts to larger clusters by using argon because of the more

(1) Philips, J. C. *Chem. Rev.* **1986**, *86*, 619.
(2) Sievert, R.; Cadez, I.; van Donz, J.; Castleman, A. W., Jr. *J. Phys. Chem.* **1984**, *88*, 4502.
(3) Squire, D. W.; Bernstein, R. B. *J. Phys. Chem.* **1984**, *88*, 4944.
(4) Jonkman, H. T.; Even, U.; Kommandeur, J. *J. Phys. Chem.* **1985**, *89*, 4240.
(5) Becker, E. W.; Bier, K.; Henkes, W. *Z. Z. Phys.* **1956**, *146*, 333.
(6) Hagena, O. F.; Obert, W. *J. Chem. Phys.* **1972**, *56*, 1793.
(7) Even, U.; de Lange, P. J.; Jonkman, H. T.; Kommandeur, J. *Phys. Rev. Lett.* **1986**, *56*, 965.
(8) Hagstrum, H. D. *Phys. Rev.* **1966**, *150*, 495.

0022-3654/88/2092-5749$01.50/0